Supporting Information

Two essential FtsH proteases control the level of the Fur repressor during iron deficiency in the cyanobacterium *Synechocystis* sp. PCC 6803

Vendula Krynická[a,b], Martin Tichý[a,b], Jaroslav Krafl [a,b], Jianfeng Yu[c], Radek Kaňa[a,b], Marko Boehm[c], Peter J. Nixon[c] and Josef Komenda[a,b,1]

[a]Institute of Microbiology, Academy of Sciences, Opatovický mlýn, 37981 Třeboň, Czech Republic

[b]Faculty of Science, University of South Bohemia, Branišovská 31, 370 05 České Budějovice, Czech Republic

[c]Department of Life Sciences, Sir Ernst Chain Building-Wolfson Laboratories, Imperial College London, South Kensington Campus, London SW7 2AZ, United Kingdom

[1]To whom correspondence should be addressed. E-mail: komenda@alga.cz

This supporting information contains:
Figures S1 to S8 and Supplementary methods and references

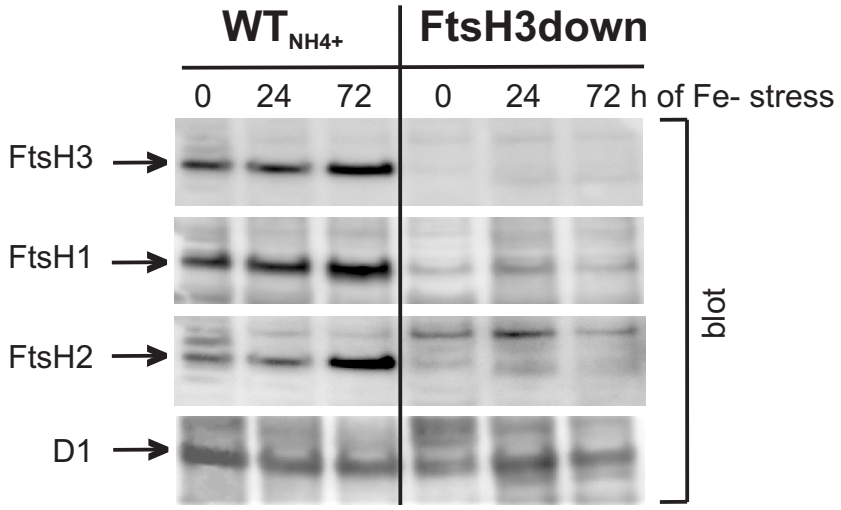

Figure S1. Changes in the level of FtsH3, FtsH1 and FtsH2 during adaptation of WT_{NH4+} and FtsH3down strains to iron starvation. Membrane proteins isolated from cells of WT_{NH4+} and FtsH3down after 0, 24 and 72 h of iron depletion were analyzed by 1D SDS-PAGE and immunoblot using antibodies against FtsH3, FtsH1 and FtsH2; immunoblot using the D1-specific antibody was used as a loading control. Each loaded sample contained 2 μg of Chl.

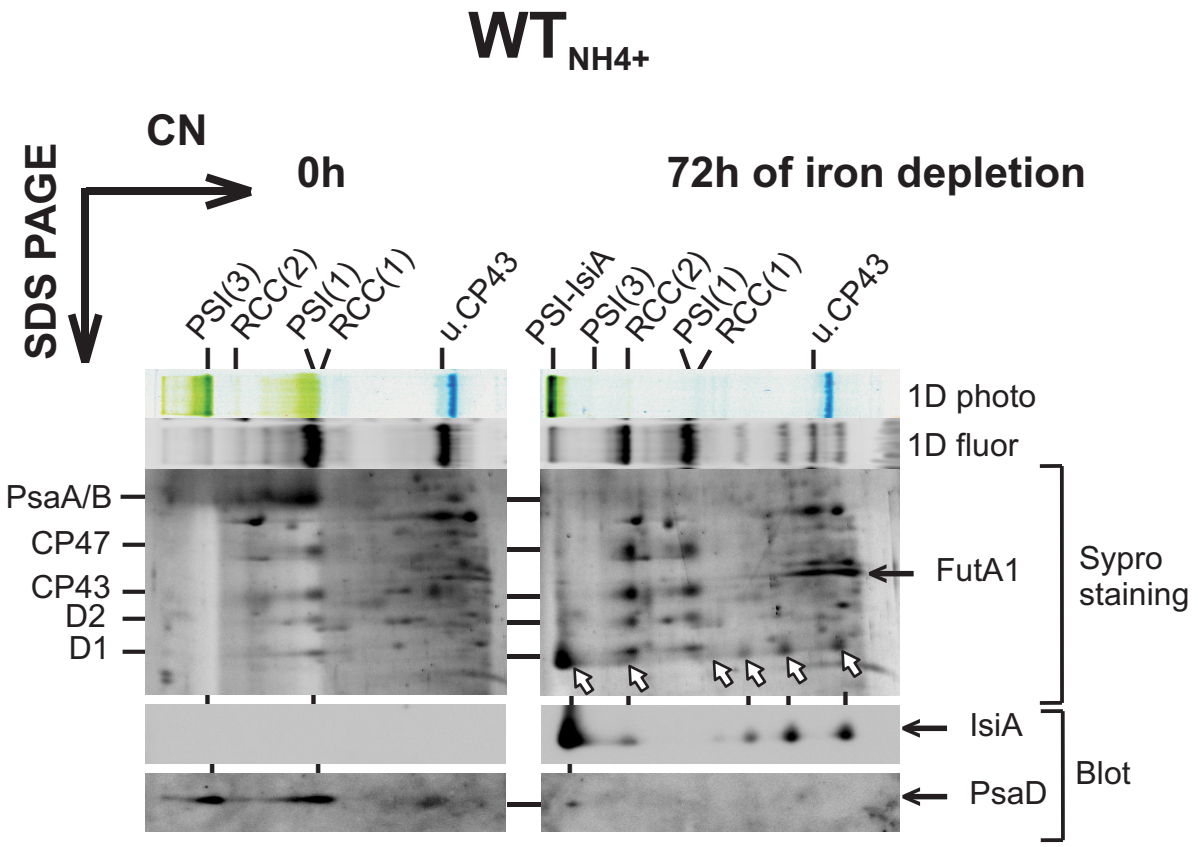

Figure S2. Detection of IsiA and PsaD proteins in cells of WT_{NH4+} before and after 72 h of iron depletion. Cells grown in the BG11NH medium were transferred to Fe– medium. Thylakoid membranes were isolated from cells harvested after 0 and 72 h of growth in Fe– medium. Membrane protein complexes were analyzed by 2D CN/SDS-PAGE. The 1D native gel was photographed (1D photo) or scanned by LAS 4000 for fluorescence (1D fluor) and after SDS-PAGE in the 2nd dimension the resulting 2D gel was stained by Sypro Orange and used for immunoblotting using specific antibodies against IsiA and PsaD proteins. Each loaded sample contained 5 µg of Chl. Designation of complexes: PSI(3) and PSI(1), trimeric and monomeric Photosystem I complexes; PSI-IsiA, supercomplexes of trimeric Photosystem I and IsiA; RCC(2) and RCC(1), dimeric and monomeric Photosystem II core complexes; u.CP43, unassembled CP43. White arrows designate IsiA protein in various complexes, black arrows FutA1. The identity of FutA1 was verified by mass spectrometry (see Table S1).

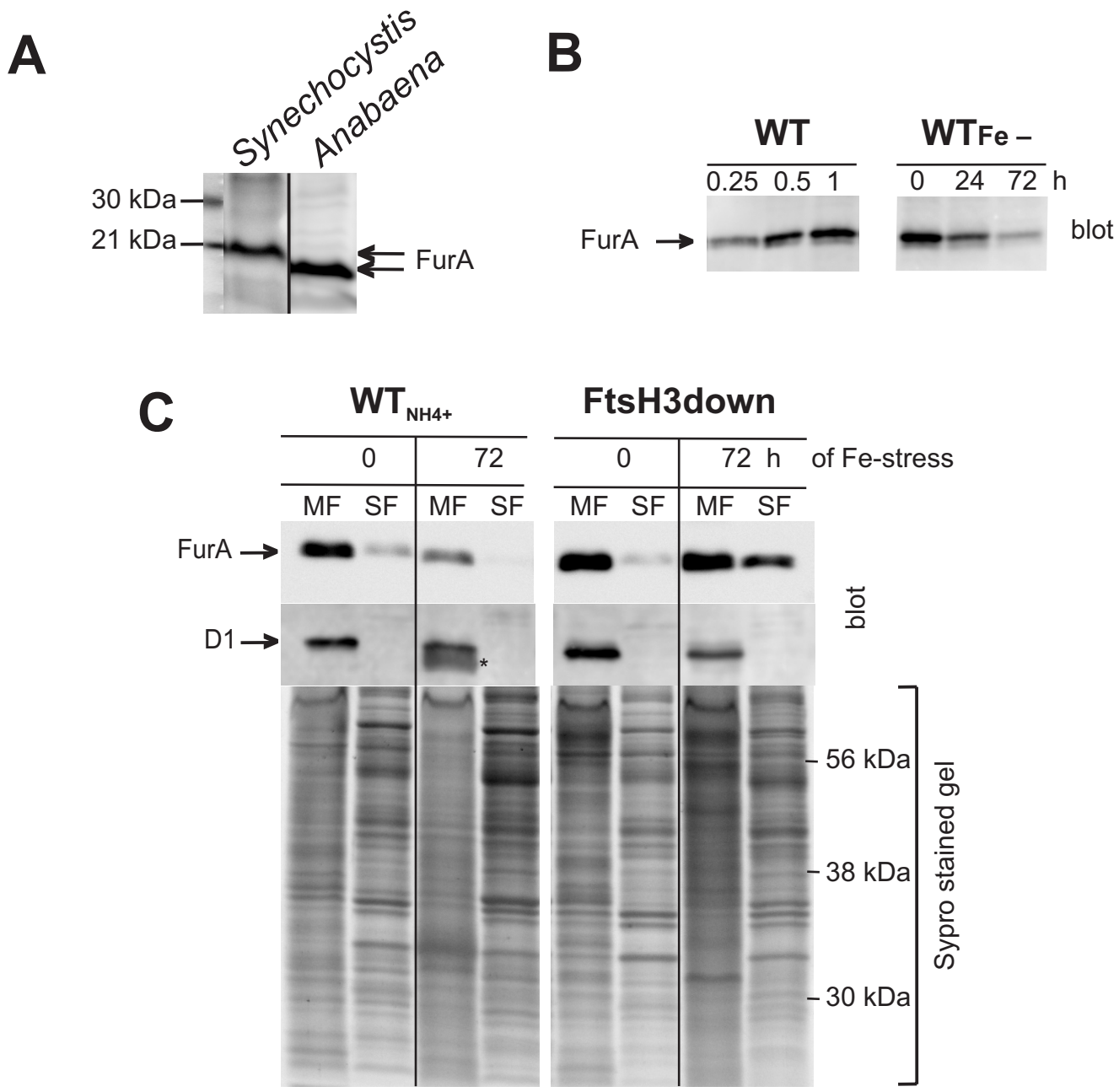

Figure S3. Detection of Fur in membranes of *Synechocystis* PCC 6803 and *Anabaena* PCC 7119 by antibody raised against Fur from Anabaena (A), detection of Fur in membranes of *Synechocystis* WT strain during iron deficiency including a dilution series of the Fur-specific antibody for control WT cells (B) and distribution of Fur between membrane and soluble fraction in WT_{NH4+} and FtsH3down cells (C). **A:** Membrane proteins isolated from cells of *Synechocystis* PCC 6803 WT and *Anabaena* PCC 7119 were analyzed by 1D SDS-PAGE and immunoblot using antibody raised against the Fur protein from *Anabaena* PCC 7119. Each loaded sample contained 2 µg of Chl. **B:** Membranes isolated from control cells of *Synechocystis* WT and diluted 1, 2 and 4 times (1, 0.5 and 0.25) were analyzed by 1D SDS-PAGE in parallel with membranes from WT cells harvested after 0, 24 and 72h of growth under iron deficiency. The gel was used for immunodetection using antibody specific for Fur to document linearity of the antibody response and decrease in the Fur level in membranes of WT. **C:** Membrane (MF) and soluble (SF) fraction isolated from the cells of WT_{NH4+} and FtsH3down mutant harvested after 0 and 72 h of iron depletion were analyzed by 1D SDS-PAGE; Gels were stained by Sypro Orange and used for immunodetection of Fur. The immunodetection of the D1 protein is shown as the membrane protein control, asterisk designates crossreaction with the strong IsiA band. Part of the Sypro-stained gel is shown to document the equal loading of the samples. Each loaded sample of MF contained 2 µg of Chl, amount of loaded SF corresponded to amount of cells containing 2 µg of Chl.

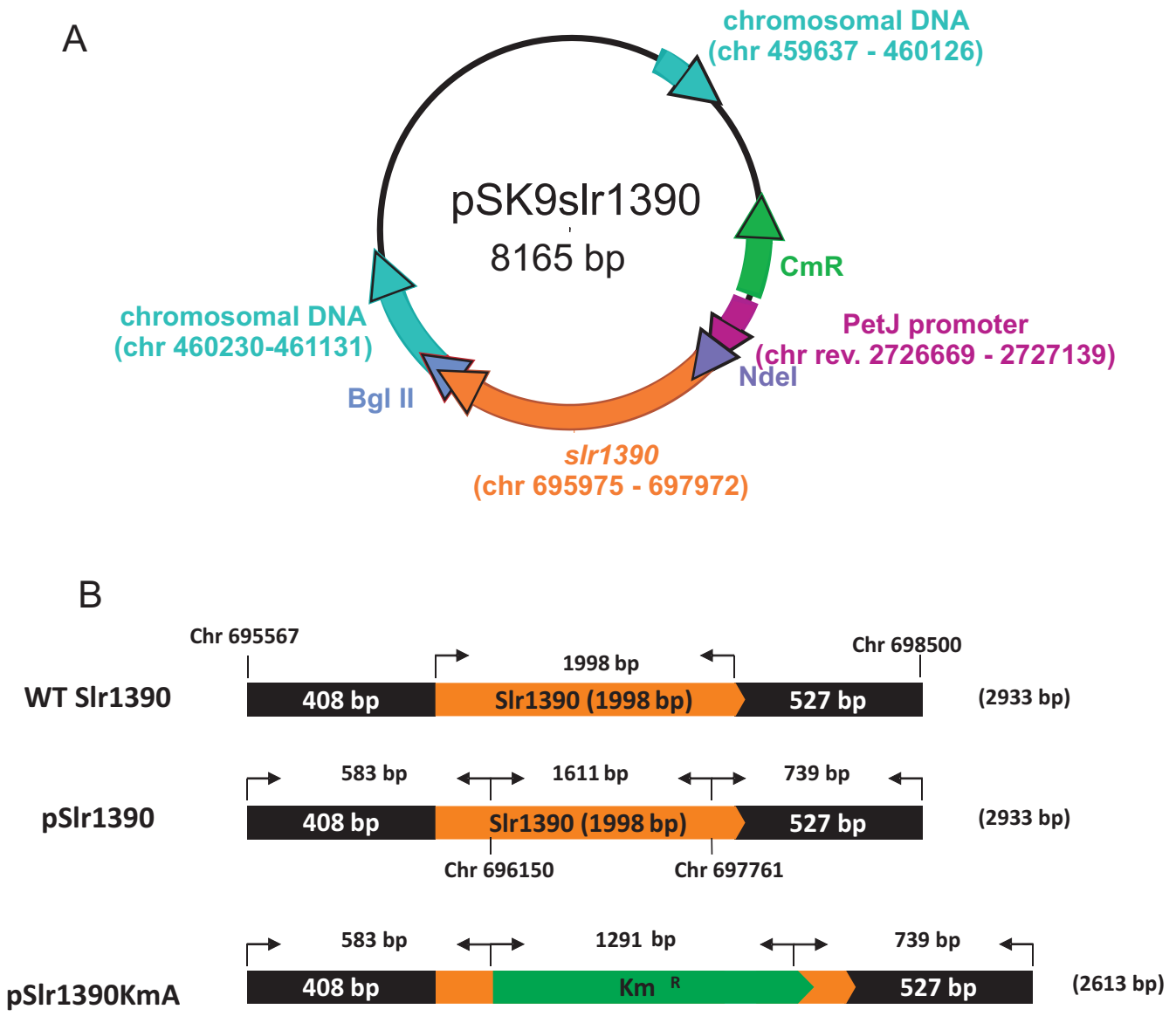

Figure S4. Construction of FtsH1down mutant. A: plasmid map of pSK9slr1390 vector used for WT transformation; B: schematic representation of FtsH1 knockout linear vector used for transformation of WTpSK9slr1390.

A

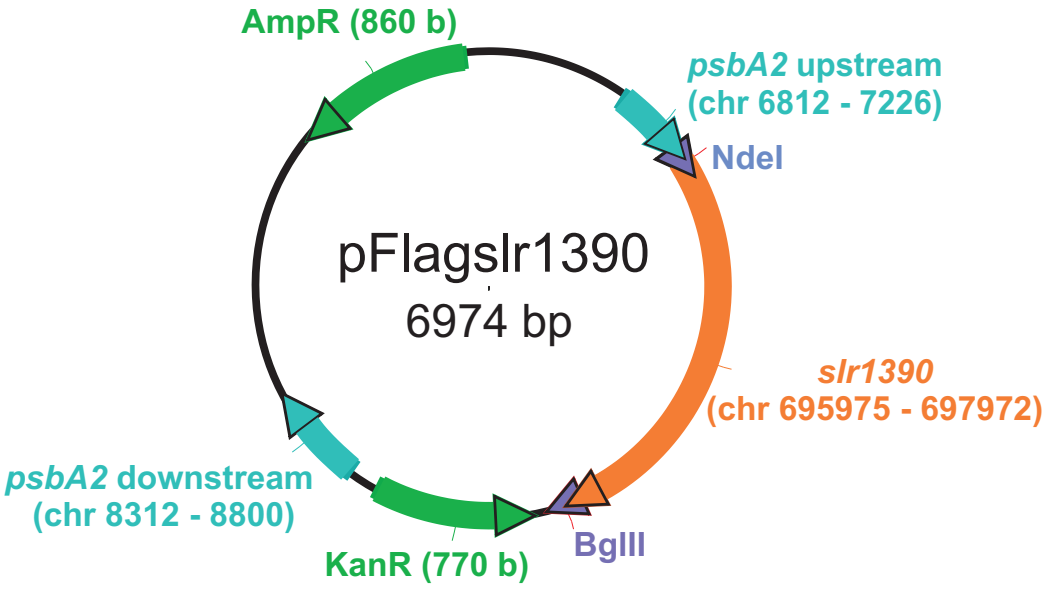

B

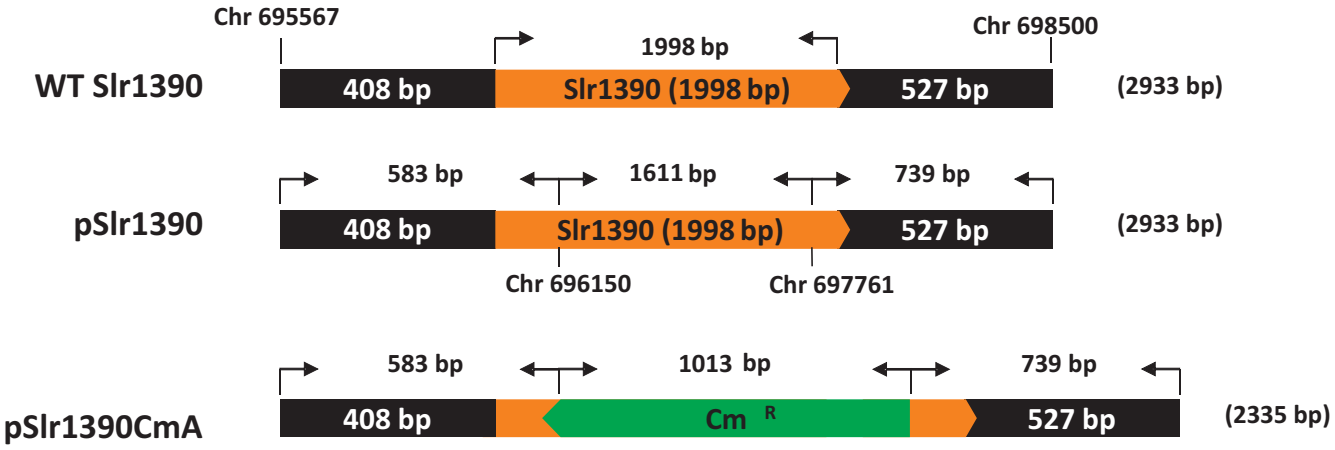

Figure S5. Construction of FtsH1over mutant. A: plasmid map of pFlagslr1390 vector used for WT transformation; B: schematic representation of FtsH1 knockout linear vector used for transformation of WTpFlagslr1390.

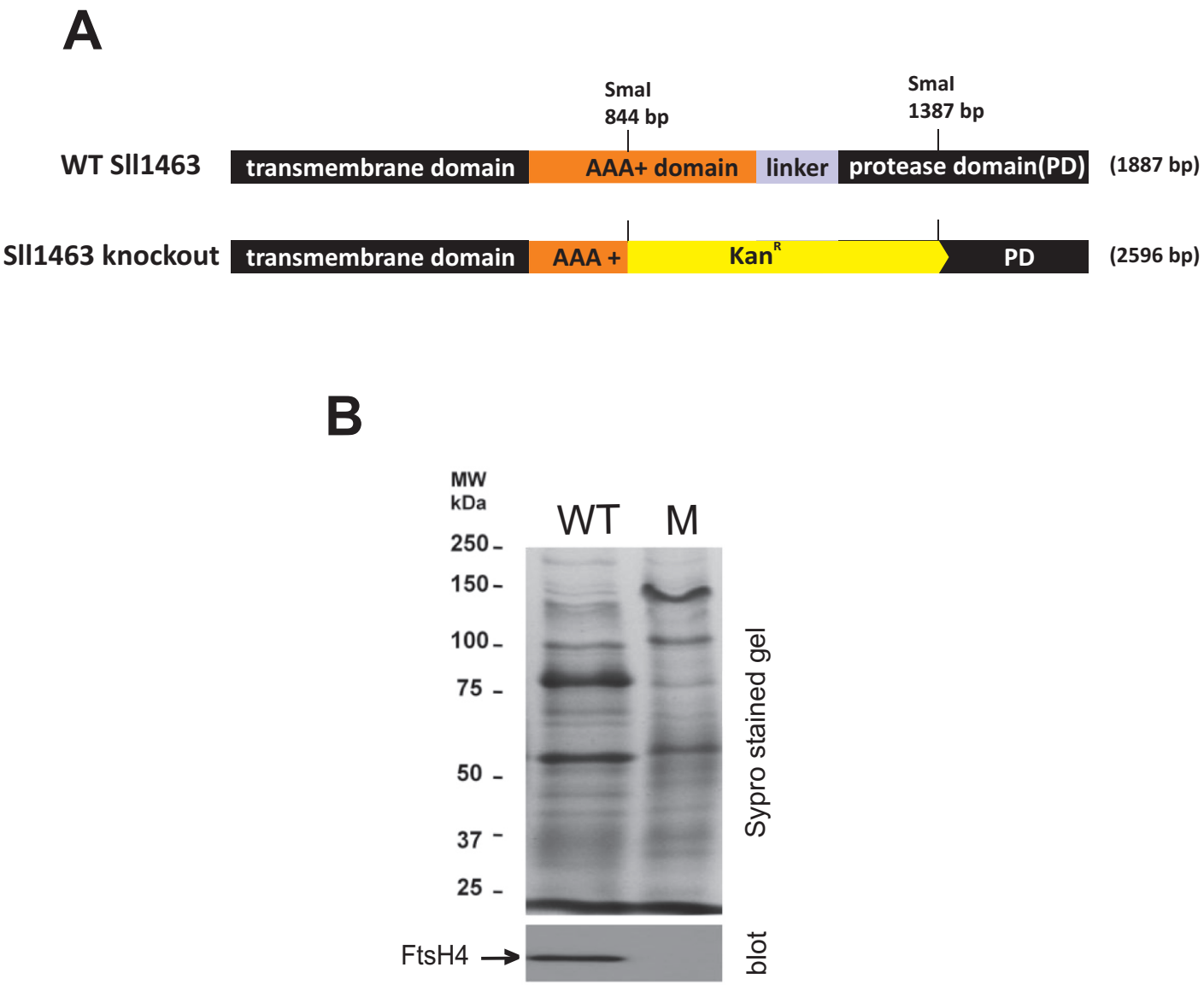

Figure S6. Construction of the FtsH2$^-$/FtsH4$^-$ knock-out mutant (A) and confirmation of the protein absence by 1D SDS PAGE (B). A: gene map of the *sll1463* gene and insertion of the kanamycin resistance cassette is shown; B: 1D SDS PAGE of membranes isolated from WT and the mutant (M); the gel was stained by Sypro Orange and used for immunodetection of FtsH4 by specific antibodies. The samples of contained 2 µg of Chl.

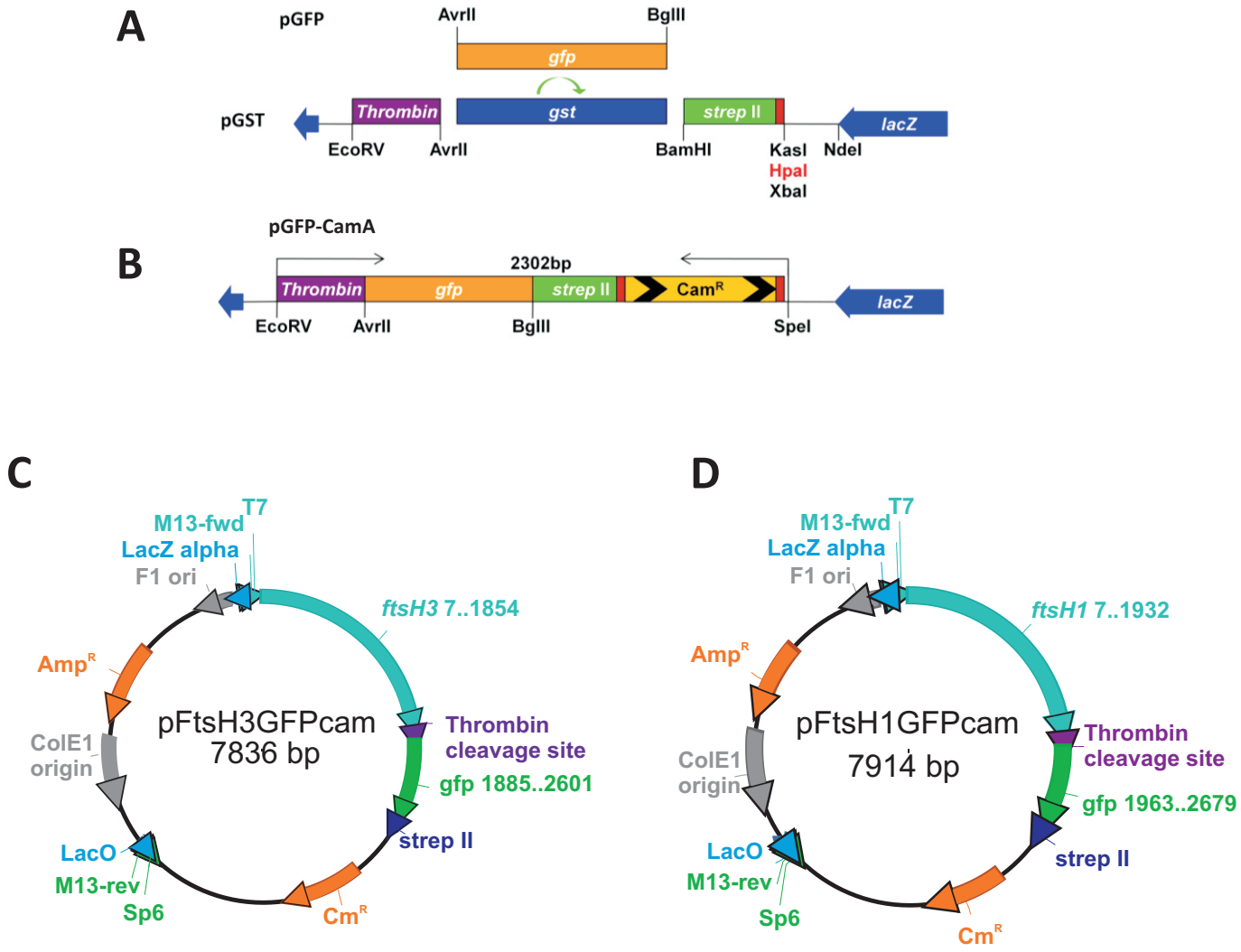

Figure S7. Construction of GFP tagging vectors. Schematic representations of the inserts found in (A) pGFP and (B) pGFP-CamA, and the plasmid map of (C) pFtsH3GFPcam and (D) pFtsH1GFPcam. A detailed description of the cloning strategy can be found in Supplementary Materials and Methods. In panels (A) and (B), blue arrows represent lacZ' on the pGEM-T Easy vector backbone. Purple boxes represent the coding sequence of the thrombin cleavage site. Orange and green boxes indicate the *gfp*:*strep* II tagging sequence. The yellow box indicates the chloramphenicol-resistance cassette; the black arrows show the direction of transcription.

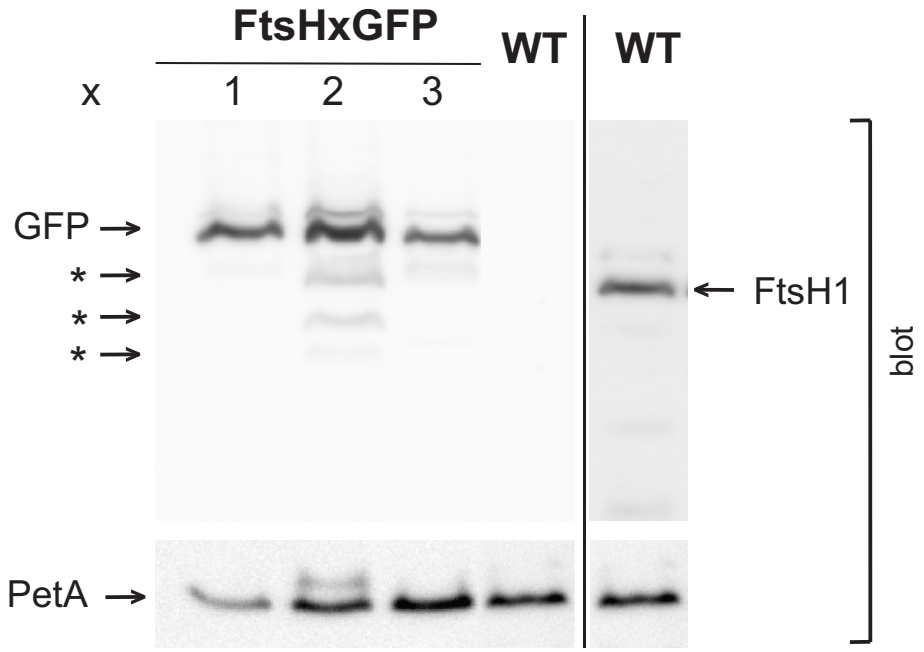

Figure S8. Accumulation of FtsH-GFP fusion proteins in membranes of strains with *ftsH1-3* genes replaced by *gfp*-tagged variants. Membranes from WT and each GFP-tagged strain were analyzed by 1D SDS-PAGE, gels were stained by Sypro Orange, and used for blotting and immunodetection using antibodies specific for GFP (left) and FtsH1 to document size of the designated proteins. Asterisks designate GFP-containing fragments. Signals of cytochrome f (PetA) are also shown to document loading of the samples. Each loaded sample contained 2 μg of Chl.

Supplementary Materials and Methods

Deleting the wild type copy of ftsH1

The wild-type copy of the *ftsH1* (*slr1390*) was deleted using linear construct containing upstream and downstream regions of the *ftsH1* gene with the kanamycin resistance cassette in the middle (Fig S4B) generated by megaprimer PCR method (Burke and Barik, 2003). In the first step, upstream and downstream regions of *ftsH1* were separately amplified using long fusion primers complementary to the *ftsH1* gene in one direction and the kanamycin cassette in the other: primer 1 (CTTCTTCACGAGGCAGACCTCAGCGCTTCTCCATTGCTG) and primer 2 (CTGTTTCCTGTGTGAAATTGTTATCATGGATTTACTAGT) (the *ftsH1* part is underlined). These fusion primers were used in pairs with *ftsH1* upstream forward and downstream reverse primers: (AAGCAATAGTCCCAATCC) and (TCATTAGTGTTGACCGAG). In the second step, the kanamycin resistance cassette (pUC4K) was amplified using PCR products from the first step as primers. Finally, the complete deletion construct was amplified using *ftsH1* upstream forward and downstream reverse primers and used for transformation of *Synechocystis* 6803 cells. Transformants were selected and segregated on kanamycin-containing agar plates; their full segregation was confirmed by PCR. For the second deletion construct, primers 1 and 2 were replaced with fusion primers complementary to the the chloramphenicol cassette primer 1‘ (CTTACTGATTTACTCTATGATGGTGCTTCTCCATTGCCTG) and primer 2‘ (GGATGAATGGCAGAAAT TCGAAAGCATGGATTTACTAGT) from pACYC184.

Construction of the FtsH2/FtsH4-less double mutant

The FtsH2/FtsH4-less double mutant complex was constructed by transformation of the existing FtsH2^{-} by a *ftsH4* knockout vector which was made in two steps. First, the entire ORF of *ftsH4* (*sll1463*) was PCR amplified with primer pair FtsH4-F1 (ATGGCCATCAAACCCCAACCCCAATGGC) and FtsH4-R1 (TTATACCACTAGGGTGCCAGGA GCTTG), the resulting PCR fragment was then ligated into pGEM-T Easy vector to create pFtsH4WT. Second, a kanamycin resistance cassette was inserted into pFtsH4WT via SmaI sites, replacing a ~550 bp *ftsH* coding sequence spanning across the AAA+ and protease domain (Fig. S6A). The resulting *ftsH4* knockout vector, namely pFtsH4-KanA, was then used to transform the FtsH2^{-} strain (Komenda *et al.*, 2006).

Construction of the FtsHxGFP strains

FtsHxGFP mutants were constructed using a universal tagging cassette consisting of the coding sequences for the thrombin cleavage site, GFP, and strep II tag and a selectable marker conferring chloramphenicol resistance (Fig. S7). The *gfp* gene was amplified from pMutin (Scholz *et al.*, 2000) using the GFP-F (GGGTCCCCTAGGATGGCTAGCAAAGGAGAAGAACTTTTCACTGGAGT) and GFP-R (AGATCTAGATCTTTTGTAGAGCTCATCCATGCCATGTGTAATCCCAGCAGCAGTT) primer pair and cloned into pGST (Boehm *et al.*, 2012) to yield the intermediate vector pGFP. A chloramphenicol resistance marker was then ligated into pGFP via the HpaI site to generate pGFPcamA. To construct the *ftsH:gfp* tagging vectors, the *gfp*-tagging cassette was released from pGFPcamA using EcoRV and SpeI (Fig. S6B), and ligated into pGEMFtsHx (Boehm *et al.*, 2012) via EcoRV and XbaI sites to yield the final transformation vectors pFtsHxGFPcam, where FtsHx is the particular FtsH subunit (Fig. S6C and D).

Fluorescence microscopy

Fluorescence micrographs were obtained with a laser-scanning confocal microscope Olympus FV1000 (Olympus, Japan). The 100x oil immersion lens were used (UPLSAPO, NA=1.4) and fluorescence was detected by a spectral detector. Before measurement, *Synechococystis sp* cells were adapted at low light (about 6 μmol m^{-2} s^{-1}) in liquid culture. Microscopic experiments were then carried out with cells fixed on a thin layer of agar, GFP and Chl fluorescence were measured simultaneously in two different channels. GFP and Chl fluorescence were excited with an Argon laser (488 nm line; 30 mW laser power, 10% used for scanning; excitation dichroic mirror 405/488/559/635), GFP fluorescence was measured between 500-530 nm (with emission dichroic mirror reflecting below 560 nm) and Chl fluorescence between 690-790 nm. Series of 20 images (512x512 pixels, a dwell time 2 μm/pixel, zoom 9.0) were taken for every sample (about image/0.5 s) that allowed us to control acquisition bleaching during experiment. The image series were exported with the Olympus FluorViewer 10-ASW software (Olympus, Japan) and further analyzed with the public domain Java image processing program ImageJ 1.45d (Abramoff *et al*., 2004). Images in the series were averaged to improve S/N ratio, GFP and Chl differences across the cell were then calculated by OriginPro 9.1 (OriginLab Corporation, Northampton, MA) to quantified GFP localization.

Supplementary References

Abramoff, M. D., Magalhães, P. J., and Ram, S. J. (2004) Image processing with ImageJ. *Biophoton. Int.* **11**: 36 - 42.

Boehm, M., Yu, J. F., Krynicka, V., Barker, M., Tichy, M., Komenda, J., *et al.* (2012) Subunit Organization of a *Synechocystis* Hetero-Oligomeric Thylakoid FtsH Complex Involved in Photosystem II Repair. *Plant Cell* **24**: 3669-3683.

Burke, E., and Barik, S. (2003) Megaprimer PCR: application in mutagenesis and gene fusion. *Methods Mol Biol* **226**: 525-532.

Komenda, J., Barker, M., Kuvikova, S., de Vries, R., Mullineaux, C. W., Tichy, M., *et al.* (2006) The FtsH protease slr0228 is important for quality control of Photosystem II in the thylakoid membrane of *Synechocystis* sp PCC 6803. *J Biol Chem* **281**: 1145-1151.

Scholz, O., Thiel, A., Hillen, W., and Niederweis, M. (2000) Quantitative analysis of gene expression with an improved green fluorescent protein. *Eur J Biochem* **267**: 1565-1570.